

# Synthesis of P1'-Functionalized Macrocyclic Transition-State Mimicking HIV-1 Protease Inhibitors Encompassing a Tertiary Alcohol

Maria De Rosa,<sup>†</sup> Johan Unge,<sup>‡</sup> Hitesh V. Motwani,<sup>†</sup> Åsa Rosenquist,<sup>§</sup> Lotta Vrang,<sup>§</sup> Hans Wallberg,<sup>§</sup> and Mats Larhed<sup>\*||</sup>

<sup>†</sup>Department of Medicinal Chemistry, Organic Pharmaceutical Chemistry, BMC, Uppsala University, P.O. Box 574, SE-751 23 Uppsala, Sweden

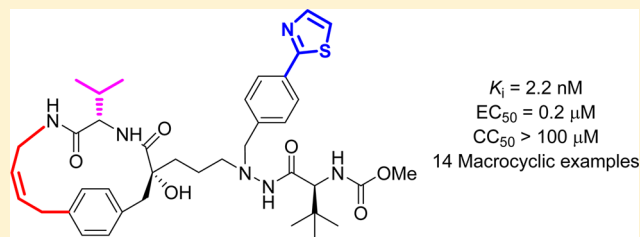
<sup>‡</sup>MAX IV-Laboratory, Lund University, P.O. Box 118, SE-221 00 Lund, Sweden

<sup>§</sup>Medivir AB, P.O. Box 1086, SE-141 22 Huddinge, Sweden

<sup>||</sup>Department of Medicinal Chemistry, Science for Life Laboratory, BMC, Uppsala University, P.O. Box 574, SE-751 23 Uppsala, Sweden

## Supporting Information

**ABSTRACT:** Seven novel tertiary alcohol containing linear HIV-1 protease inhibitors (PIs), decorated at the *para* position of the benzyl group in the P1' side with (hetero)aromatic moieties, were synthesized and biologically evaluated. To study the inhibition and antiviral activity effect of P1–P3 macrocyclization, 14- and 15-membered macrocyclic PIs were prepared by ring-closing metathesis of the corresponding linear PIs. The macrocycles were more active than the linear precursors and compound **10f**, with a 2-thiazolyl group in the P1' position, was the most potent PI of this new series ( $K_i$  2.2 nM,  $EC_{50}$  0.2  $\mu$ M). Co-crystallized complexes of both linear and macrocyclic PIs with the HIV-1 protease enzyme were prepared and analyzed.



## INTRODUCTION

Antiretroviral therapy (ART) has markedly changed the outcome for HIV-infected patients.<sup>1</sup> Gratifyingly, there were more than 700000 fewer new HIV infections globally in 2011 than in 2001. However, the emergence of resistance strains continues to impact the efficacy of current antiretroviral regimens.<sup>2</sup> The road from 2.5 million new HIV infections in 2011 to nearly zero new HIV infections is still very long, and a significant effort is required to further develop the existing HIV prevention programmes.<sup>3</sup>

HIV-1 protease inhibitors (PIs) are essential components in the therapeutic treatment against HIV, but their use is somewhat limited by severe side effects such as dyslipidaemia and hypersensitivity.<sup>4,5</sup> Peptide-derived drugs are also known to suffer from metabolic instability<sup>6</sup> and poor membrane permeation,<sup>7</sup> which mainly arise due to the presence of peptide bonds, high conformational flexibility and the exposure of polar functionalities in linear molecules. Macrocyclization of linear peptides represents an important approach to overcome this problem.<sup>8</sup>

There has been large interest in both naturally occurring and synthetic cyclic peptides as scaffolds in drug discovery efforts.<sup>9,10</sup> A macrocyclic peptide provides diverse functionality, increased structural rigidity, and large stereochemical complexity in a preorganized ring structure.<sup>8</sup> Preorganization will favor

improved affinity for protein targets by reducing the entropy loss upon binding.<sup>11</sup> Furthermore, cyclizations may provide better resistance to proteolytic digestion and facilitate internal hydrogen bonding, thus helping to improve bioavailability and enable the compound to reach its intracellular targets.<sup>12</sup>

Recently, we have applied the macrocyclization strategy for preparing a new series<sup>13</sup> of HIV-1 PIs related to atazanavir<sup>14,15</sup> but containing a tertiary alcohol as part of the transition-state mimicking core structure (Figure 1).<sup>13,16</sup>

Cyclic PIs with bromine in the *para*-position of the P1' were up to 15 times more potent in the cell assay as compared to the linear precursors, exhibiting  $EC_{50}$  values down to 370 nM.<sup>13</sup> Although the best macrocycles had lower  $EC_{50}$  values than the corresponding linear PIs, the differences at the enzyme level ( $K_i$ ) were not impressive. X-ray crystallography data suggested that the P1–P3 sites of both linear and macrocyclic PIs accommodate the lipophilic pockets of the enzyme in the same fashion.<sup>13</sup> Therefore, we decided to explore deeply the structure–activity–relationships (SARs) of the linear molecule–enzyme interactions to optimize the PIs in the P1' position and to investigate the macrocyclization strategy further to obtain new potential anti-HIV compounds with both

Received: March 19, 2014

Published: July 23, 2014

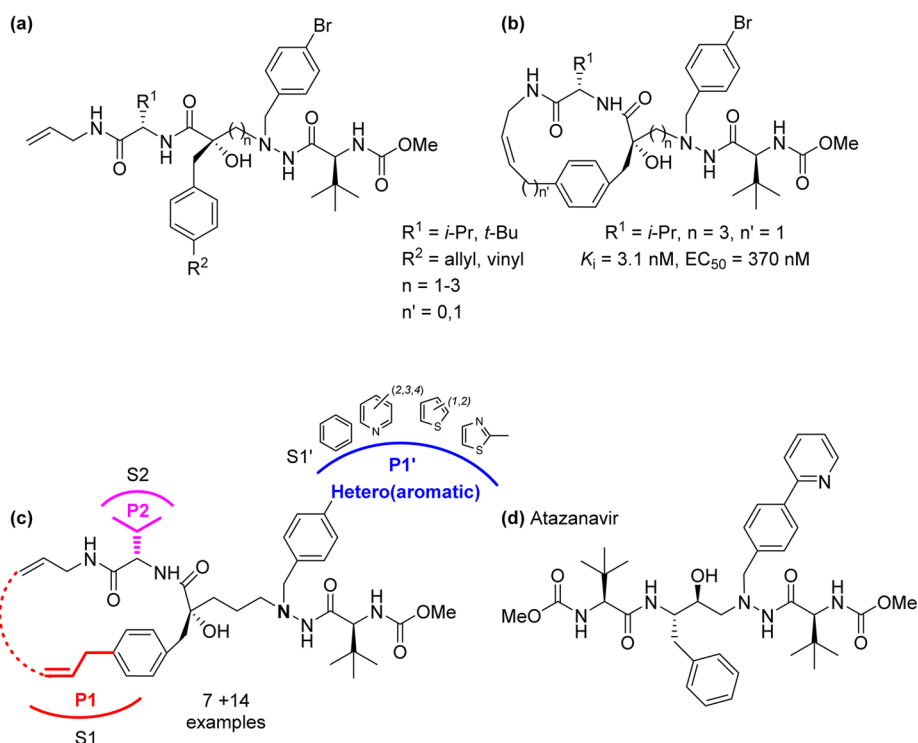


**Figure 1.** (a) General structure of reported linear PIs encompassing a tertiary alcohol,<sup>16</sup> (b) general structure of reported macrocyclic PIs,<sup>13</sup> (c) general structure of the new series of linear and macrocyclic PIs functionalized in the P1' position, (d) atazanavir.

improved potency ( $EC_{50}$ ,  $K_i$ ) and pharmacokinetic profile. We herein report the synthesis, biological evaluation, and crystallography data of two new series, linear and 14–15-membered P1–P3 macrocyclic PIs, encompassing a tertiary alcohol in the transition-state mimicking scaffold and various (hetero)aromatic substituents in the *para*-position of the P1' side chain (Figure 1c).

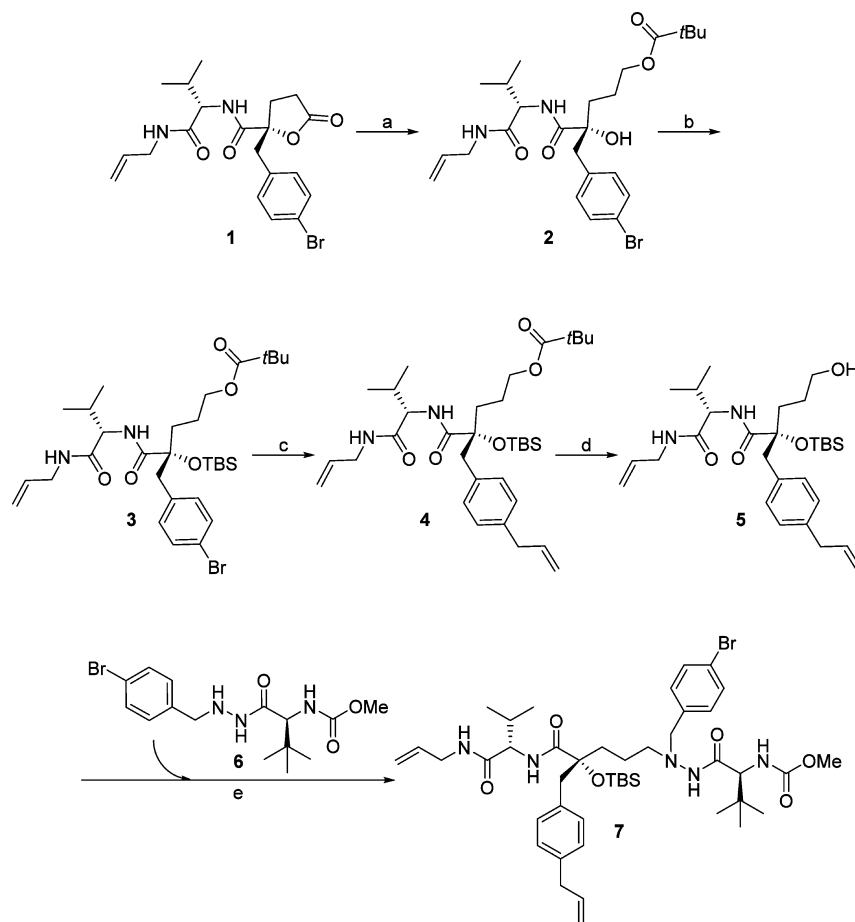
## RESULTS

**Chemistry.** Compound **1** was synthesized as previously reported<sup>13</sup> and used as the starting material for the preparation of the new PIs. The lactone moiety of compound **1** was reduced using lithium borohydride, and the newly formed primary alcohol was selectively protected as a pivalate ester to give **2** in good yield of 70% over two steps. The tertiary alcohol was thereafter protected using *tert*-butyldimethylsilyl triflate affording intermediate **3**. The bromine in 4-position of the aryl bromide **3** was substituted with an allyl group using a Stille coupling reaction<sup>17,18</sup> to provide compound **4** in high yield of 75% (Scheme 1). Reaction of ester **4** with lithium borohydride yielded intermediate primary alcohol **5** (85%), which was oxidized using Dess–Martin reagent to the corresponding aldehyde. This was followed by a reductive amination with the hydrazide **6**<sup>19</sup> using a catalytic amount of acetic acid to activate the aldehyde and sodium triacetoxyborohydride as the reductive agent in a one-pot procedure to obtain **7** (44% over three steps). Compound **7** was thereafter used as precursor for the preparation of the linear series of new PIs diversely substituted at the P1' side chain. The 4-position of the benzyl moiety was decorated with phenyl-, pyridyl-, thienyl-, and thiazolyl groups.

The 4- and 3-pyridyl moieties were introduced via microwave assisted<sup>20</sup> Suzuki–Miyaura cross-coupling reactions (Scheme 2a) using the corresponding boronic acids, Herrmann's

palladacycle (as a palladium precatalyst) together with potassium carbonate as base and the preligand tri(*tert*-butyl)phosphonium tetrafluoroborate in dimethoxyethane/water<sup>21–23</sup> to obtain **8a–b** in moderate to high isolated yields (54–78%). Unfortunately, this protocol was not successful when phenyl-, thienyl-, and thiazolylboronic acids were used. Hence, an alternative protocol using palladium(II) acetate as precatalyst, 2 M aqueous solution of sodium carbonate as base, and triphenylphosphine as ligand in dimethoxyethane/ethanol and irradiating the reaction vial in a microwave reactor was chosen.<sup>24</sup> The desired products (**8c–e**) were obtained in high isolated yields (70–85%).

The functionalization of precursor **7** via Suzuki cross-coupling reaction with 2-(pyridyl/thiazolyl)boronic acids was not successful, possibly due to rapid protodeboronation, oxidation, and/or polymerization.<sup>25–27</sup> In an effort to combat this problem, several attempts were made using the corresponding *N*-methyliminodiacetic (MIDA) esters<sup>28</sup> of the above-mentioned boronic acids. The reactions were performed using temperatures in the range of 85–130 °C and investigating different amount of base for the in situ hydrolysis of the MIDA esters but without any positive outcome. In all attempts, an isocyanate byproduct was generated by a  $\beta$ -elimination reaction at the carbamate function in P2' position, according to LC-MS analysis and <sup>1</sup>H NMR.<sup>29</sup> Stille coupling reactions<sup>16b</sup> were also tried as a possible alternative using 2-(tributylstannyl)pyridine, but unfortunately only the starting material **7** was recovered. Thus, to introduce the 2-pyridyl and 2-thiazolyl moieties in P1' position, a different approach was chosen (Scheme 3a). Commercially available benzaldehydes **15** and **16** were reacted with hydrazide **17** to obtain the hydrazides **18a–b**.<sup>30</sup> Subsequent reaction of hydrazides **18a–b** with the primary alcohol **5** via a reductive amination process afforded the desired *tert*-butyldimethylsilyl (TBS)-protected compounds **8f–g**.

Scheme 1. Synthesis of Precursor 7<sup>a</sup>

<sup>a</sup>Reagents and conditions: (a) (i) 2 M LiBH<sub>4</sub> in THF, rt, 15 h, (ii) pivaloyl chloride, anhydrous pyridine, anhydrous DCM, rt, 17 h, 70% (over two steps); (b) TBDMS triflate, TEA, anhydrous DCM, rt, 16 h, 92%; (c) Pd(PPh<sub>3</sub>)<sub>2</sub>Cl<sub>2</sub>, CuO, allyltributylstannane, anhydrous DMF, MW, 150 °C, 30 min, 75%; (d) 2 M LiBH<sub>4</sub> in THF, 0 °C to rt, 16 h, 85%; (e) (i) Dess–Martin periodinane, anhydrous DCM, rt, 2 h, (ii) cat. AcOH, **6**, DCE, 4 h, rt, (iii) NaBH(OAc)<sub>3</sub>, rt, 18 h, 44% (over three steps).

Removal of the TBS group in compounds **8a–g** (Schemes 2b and 3c), using 1 M tetrabutylammoniumfluoride solution in THF at room temperature, furnished the desired linear PIs **9a–g** in high yields (55–95%).

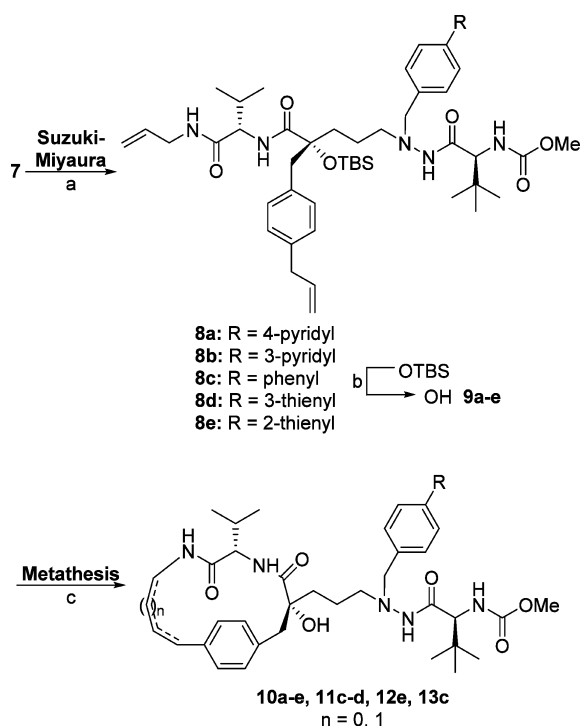
Macrocyclization of linear PIs (**9a–e**, Scheme 2c; **9f–g**, Scheme 3d) was thereafter performed via a microwave-induced ring-closing metathesis (RCM) reaction using second-generation Hoveyda–Grubbs catalyst (20 mmol %) in anhydrous dichloromethane at 130 °C.<sup>31,32</sup> Lowering the temperature (60–110 °C) and the catalyst loading (5–10 mmol %) resulted in no or only partial conversion of starting materials **9a–g**, indicating the need for higher temperature and amount of catalyst. In some cases, double-bond migration and ring contraction reactions also occurred.<sup>33–35</sup> Figure 2 depicts the outcome of RCM for all linear PIs (**9a–g**). Macrocyclization of compounds **9a–b** bearing a 4- and 3-pyridyl moiety at P1' provided the cyclic 15-membered products **10a–b** with high selectivity in good yields (57% and 54%, respectively) after 30 min of irradiation at 130 °C. For the linear compound **9c** with a phenyl group at P1', three products were isolated under identical reaction conditions, namely a ring closed product **10c**, a double-bond migrated cyclic structure **11c**, and a contracted 14-membered cyclic product **13c**. Macrocyclization of **9g** was the only reaction that did not give the expected 15-membered ring product, instead double-bond migration (**11g**) and ring

contraction (**13g**) products were obtained. These results lead us to believe that the nature of the substituent at P1' somehow influences the outcome of the metathesis toward different degrees of ring closure, double-bond migration, and ring contraction. The position of the double bond in the ring and its *Z* configuration were assigned by NMR data and X-ray data.

**Biological Evaluation: HIV Protease Inhibition, MT4 Cell-Based Anti-HIV Activity, Permeability, and Metabolic Stability in Vitro.** HIV-1 protease inhibition and cell-based antiviral activity of the newly synthesized linear and macrocyclic PIs were evaluated (Tables 1 and 2, respectively), and the corresponding *K<sub>i</sub>* and EC<sub>50</sub> values are presented.

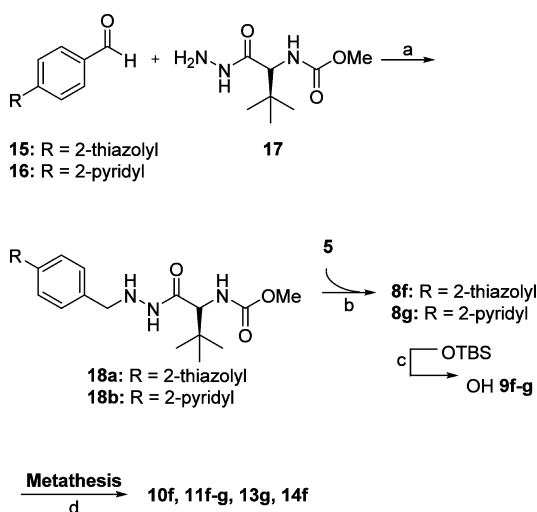
All PIs displayed good inhibition profile having *K<sub>i</sub>* in the low nanomolar range (2.2 nM ≤ *K<sub>i</sub>* ≤ 120 nM) and EC<sub>50</sub> down to 0.13 μM. We hypothesized that the introduction of varying moieties at the P1' position, with different polarity and hydrogen bonding potential, could improve the protease–inhibitor interaction in the lipophilic S1/S1' enzyme region and thus enhance the inhibition potency of the respective PIs.<sup>16c</sup> Interestingly, out of the seven linear PIs (Table 1), four were equally or more active than the corresponding bromide analogue **A** (7.8 nM ≤ *K<sub>i</sub>* ≤ 18 nM vs *K<sub>i</sub>* 30 nM for bromide analogue **A**), meaning that the P1' functionalization was well tolerated and fitted nicely into the S1' hydrophobic pocket. Gratifyingly, an improvement was also observed in anti-HIV

**Scheme 2. Synthesis of Linear PIs 9a–e and Macrocytic PIs 10a–e, 11c–d, 12e, and 13c<sup>a</sup>**



<sup>a</sup>Reagents and conditions: (a) Herrmann's palladacycle,  $K_2CO_3$ , aryl boronic acid,  $[HP(tBu)_3]BF_4$ , DME/water, MW, 140 °C, 30 min, 54–78% or  $Pd(OAc)_2$ ,  $PPh_3$ , aryl boronic acid, 2 M  $Na_2CO_3$ , DME/EtOH, MW, 130 °C, 20 min/1 h, 70–85%; (b) 1 M TBAF in THF, 0 °C to rt, 2 h, 70–95%; (c) second-generation Hoveyda–Grubbs catalyst, anhydrous DCM, MW, 130 °C, 1 h, 13–57%.

**Scheme 3. Synthesis of Linear PIs 9f–g and Macrocytic PIs 10f, 11f–g, 13g, and 14f<sup>a</sup>**



<sup>a</sup>Reagents and conditions: (a) (i) ethanol, reflux, 5 h, 70–80%, (ii)  $H_2/Pd-C$ , methanol, 48 h, 55–60%; (b) (i) Dess–Martin periodinane, anhydrous DCM, rt, 2 h, (ii) cat. AcOH, 5, DCE, 4 h, rt, (iii)  $NaBH(OAc)_3$ , rt, 18 h, 44–49% (over three steps); (c) 1 M TBAF in THF, 0 °C to rt, 2 h, 55–65%; (d) second-generation Hoveyda–Grubbs catalyst, anhydrous DCM, MW, 130 °C, 1 h, 15–30%.

cellular activity, as all new linear PIs exhibited  $EC_{50}$  lower ( $EC_{50} \leq 3.7 \mu M$ ) than the bromide analogue A ( $EC_{50} 6.0 \mu M$ ).<sup>13</sup> PI

**9a** with a 4-pyridyl moiety in P1' position was the best linear PI of this new series, having a  $K_i$  value of 7.8 nM (Table 1) and  $EC_{50}$  value of 0.81  $\mu M$ . Introduction of a phenyl group (**9c**) or a 3-thiophene group (**9d**) was not as beneficial because less potent PIs were obtained ( $K_i$  65 and 64 nM, respectively) although with slightly better antiviral activities (3.7  $\mu M$  for both PIs vs 6.0  $\mu M$  for A). Activity of PI **9e** carrying a 2-thiophene substituent on the P1' side chain seemed to be quite similar to the bromide analogue ( $K_i$  35 nM vs 30 nM and  $EC_{50}$  2.4  $\mu M$  vs 6.0  $\mu M$ , respectively, of **9e** vs A). The thiazole structure (**9f**,  $K_i$  8.0 nM) was almost as potent as **9a** in the enzyme assay but with a somewhat poor antiviral activity ( $EC_{50}$  2.2  $\mu M$ ).

The P1–P3 macrocyclization approach furnished in almost all cases improved PIs in terms of inhibition potency and antiviral activity (Table 2), providing  $K_i$  values in the range of 2.2–31.5 nM and  $EC_{50}$  in the range of 0.13–3.05  $\mu M$ . Macrocycle **12e** was the only exception; it was the least potent PI in this series with ( $K_i$  120 nM and  $EC_{50}$  7.35  $\mu M$ ). Table 2 also includes corresponding values of the bromide precursor **B**<sup>13</sup> and FDA approved atazanavir for comparison. Because our previous results showed that 14-membered macrocyclic PIs are less potent,<sup>13</sup> 15-membered macrocyclic rings were synthesized in the present study by using the allyl group at 4-position of the P1 nonprime side. In addition to the desired 15-membered cyclic compounds, double-bond migrated isomeric structures and ring-contracted 14-membered compounds were also formed during the metathesis reaction (Figure 2 and Table 2).<sup>33–35</sup> As expected, 14-membered ring macrocycles were in all cases less potent than the corresponding 15-membered cyclic PIs (comparing **13c** to **10c/11c**, **14f** to **10f/11f**, and **13g** to **11g**). Double-bond migration from 2,3- to the 1,2- position of the 15-membered ring macrocycles did not strongly affect the inhibition profile, as PIs with similar  $K_i$  values were observed (comparing **10c** to **11c**, **10d** to **11d**, and **10f** to **11f**). It might, though, be worth noting that when double-bond migration occurred to the 3,4-position of the 15-membered ring (**12e**,  $K_i$  120 nM), the inhibiting potency dramatically dropped nearly 7-fold (**10e** vs **12e**). Molecules **10f** and **11g**, with 2-thiazolyl and 2-pyridyl groups, respectively, were highly potent PIs of the macrocyclic series and slightly more active than the bromide precursor **B**; **10f** was the best PI ( $K_i$  2.2 nM), with very good antiretroviral activity ( $EC_{50}$  0.2  $\mu M$ ). A few PIs were also evaluated in selected in vitro resistant HIV-1 isolates and the  $EC_{50}$  values are shown in the Tables 1 and 2. Saquinavir resistant virus containing A71V, I84V and L90M mutations and ritonavir resistant virus containing M46I, V82F, and I84V mutations were isolated and used for cross resistance studies (cf. Supporting Information). Antiviral activity of atazanavir against the same mutants is also shown for comparison. The tested linear PIs were moderately active against mutations A71V, I84V, L90M, and inactive against mutations M46I, V82F, and I84V. The tested cyclic PIs exhibited equipotent activity in these mutant MT4/HIV-1 protease assays with a better inhibition profile against A71V, I84V, and L90M mutations. In general, macrocyclization improved inhibition potency on mutated HIV-1 protease. The cytotoxicity ( $CC_{50}$ ) and Caco-2 permeation ( $P_{app}$ )<sup>36</sup> and metabolic stability ( $Cl_{int}$ ) were also evaluated (cf. Supporting Information), and the results are summarized in Tables 1 and 2. Rewardingly, all new 21 PIs showed lower MT4 cell toxicity than atazanavir. All three Caco-2 tested linear PIs (**9a**, **9f**, and **9g**, Table 1) showed high permeation ( $P_{app}$  of 22–47  $\times 10^{-6}$  cm/s). When the linear PIs were cyclized, unfortunately, somehow the permeation

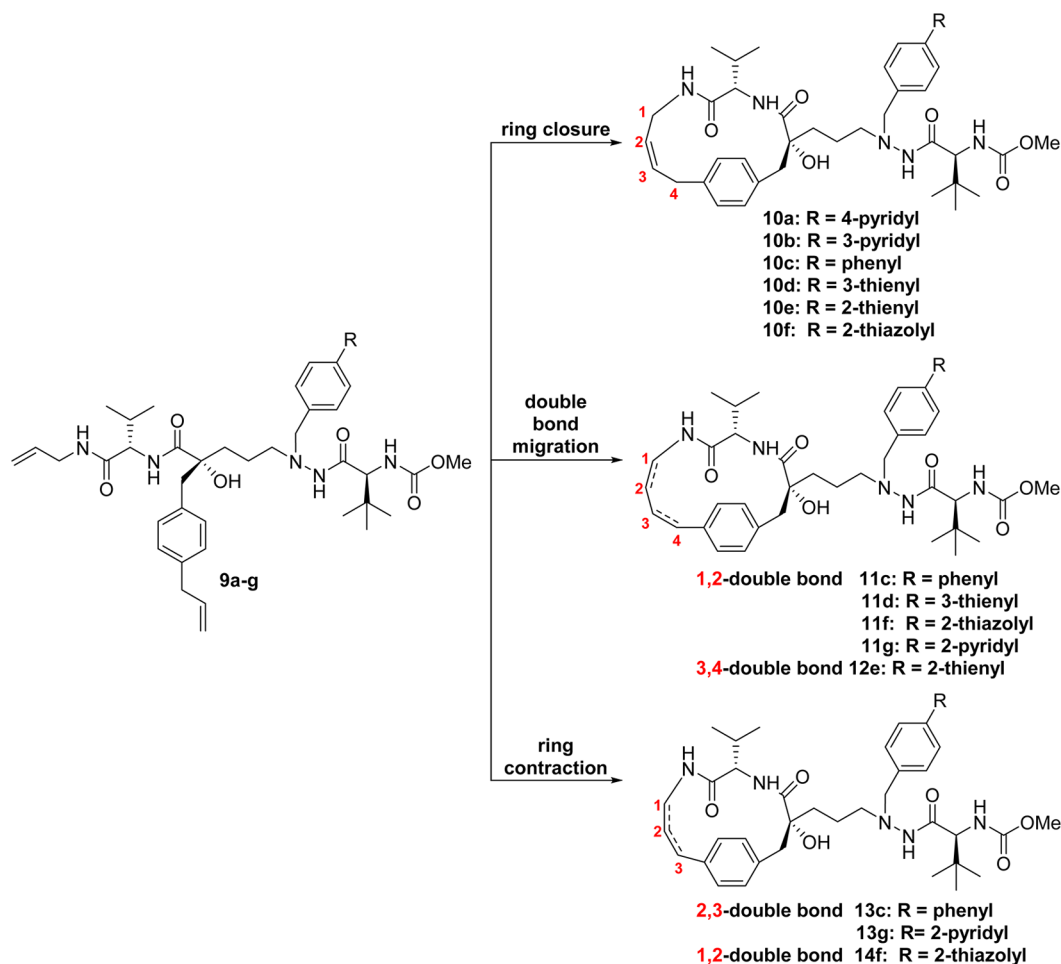


**Figure 2.** Outcome of ring closing metathesis reaction.

decreased (Table 2). Nevertheless, all measured cyclic PIs showed single- or double-digit  $P_{app}$  values similar to or higher than those of atazanavir, except for the 4-pyridine derivative **10a**. Further, all four PIs tested for the metabolic stability showed very good clearance. As expected, the macrocyclic PI **10a** ( $Cl_{int} > 300 \mu\text{g}/\text{min}/\text{mg}$ ) was more stable than the corresponding linear PI **9a** ( $Cl_{int} 73 \mu\text{g}/\text{min}/\text{mg}$ ). Both linear (**9f**) and macrocyclic (**10f**) PIs, having a thiazole moiety at the P1' position, showed similar metabolic stability ( $Cl_{int} > 300 \mu\text{g}/\text{min}/\text{mg}$ ). In general, the macrocycles showed a better intrinsic clearance when compared to atazanavir ( $Cl_{int} 90 \mu\text{g}/\text{min}/\text{mg}$ ), indicating that the macrocyclization approach can improve the metabolic stability of peptide-like molecules.

In summary, macrocyclization resulted in a consistent improvement of antiretroviral activity, in several cases similar to atazanavir. Further, the cytotoxicity property for most macrocyclic PIs was better than for the linear PIs, while the permeability was reduced from high/very high to moderate/high; however, the metabolic stability was very good.

**X-ray Structure Analysis.** X-ray crystallography data were obtained for nine new HIV-1 PI–enzyme complexes. The resolution for all complex structures were in the range of 1.5–2.45 Å. Refinement were straightforward for all structures and  $R_{free}$  around 20% for most structures with a few exceptions (cf. Supporting Information). The density was continuous in most areas of the HIV-1 PIs, which made the modeling smooth. Exceptions were observed at the P1' moiety, where the atoms of the heterosubstituted outermost ring, in most of the

complexes, had a limited density map. Nonetheless, the electron density maps suggested a good fit to the data and the orientation could be easily sorted out for all complexes. In our previously published work, the linear PIs carrying a vinylic or allylic P1 substituent failed to give good crystallography data.<sup>13</sup> With the set of nine structures presented in this study, a detailed comparison of linear and macrocyclic scaffolds was carried out. Current data set has helped to analyze the global effect of the P1–P3 macrocyclization approach on the binding profile of the PIs. The two different scaffolds (linear and macrocyclic) bind similarly to the enzyme, with only minor differences (Figure 3). The main effect of the macrocyclization seems to be that the introduced constraints make the macrocycles slightly smaller than the corresponding linear PIs, which allowed small adjustments and a better fit of the macrocycles in the P1–P3 pockets. Interestingly, this better accommodation of the macrocyclic structures at the nonprime site of the enzyme affects the hydrogen bonding distances between the tertiary hydroxyl group of the PIs and the aspartic residues Asp25/Asp125 and Gly27 of the active site of the enzyme (Figure 4). The strengths of these bonds are of particular interest because they mimic the bonds formed during the catalytic reaction.

All macrocyclic PIs exhibited hydrogen bonds shorter than 3.0 Å (strong interaction) between the tertiary hydroxyl group and the carboxylate oxygen of Asp125. The distances between the tertiary hydroxyl group and the carbonyl oxygen Gly27 were found to be longer than 3.0 Å, indicating a less favorable

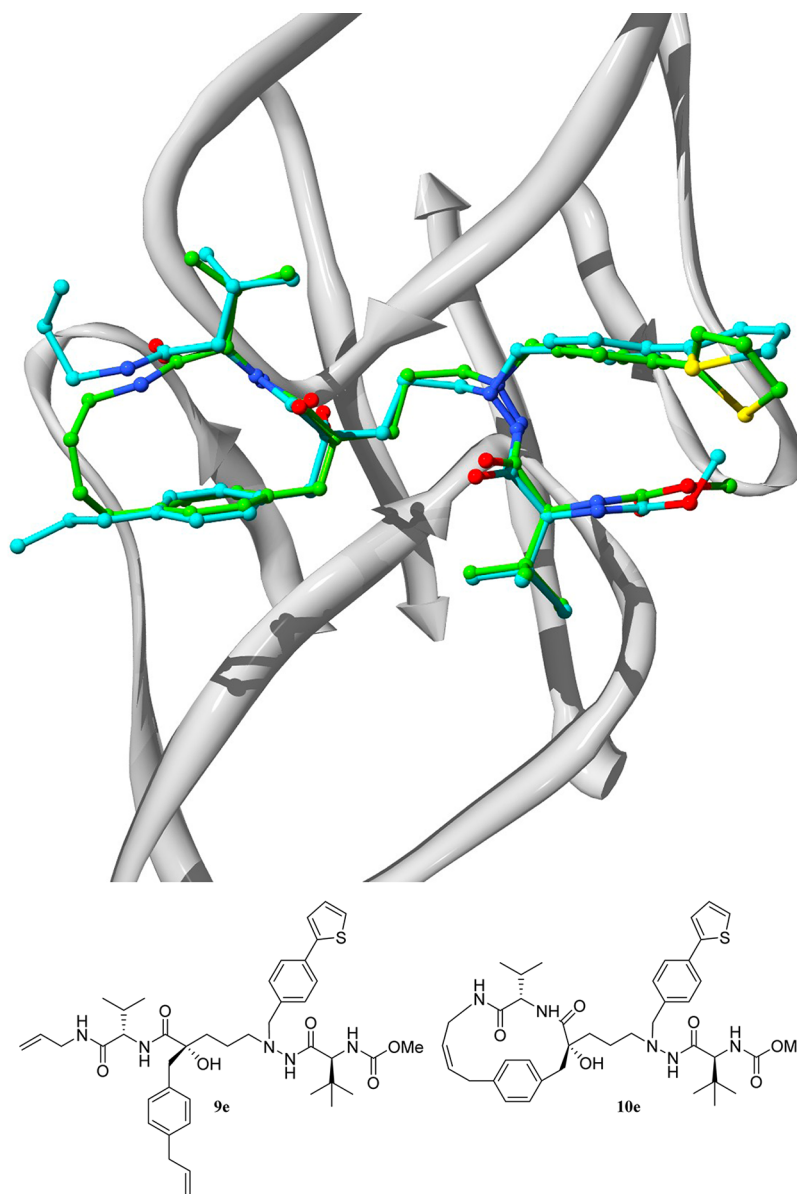


**Figure 3.** Comparison of the noncyclic PI **9e** (PDB ID 4cpr, turquoise) and the corresponding macrocycle **10e** (PDB ID 4cpx, green) complexes. The macrocyclic compound mimicked the binding of the linear PI very well, differing significantly only at the point of macrocyclization at the S3 site and at the thiophene substituent at the S1' site, the latter having partial rotational freedom. The macrocycle in nonprime side has a somewhat smaller ring structure which allows small shifts of the arrangement between several macrocyclic PIs and their linear counterparts.

bonding. The PIs **10b**, **10d**, and **10e** (PDB IDs 4cpt, 4cpu, and 4cpx, respectively) had the most favored hydrogen bond lengths, 2.7 Å, to the catalytic aspartic residues Asp125. The bond lengths for the linear scaffold on the other hand are shifted. In the **9e** complex, the bonds to Asp125 are all greater than 3.0 Å and less than 2.7 Å for the bond to the Gly27 carbonyl oxygen. The two exceptions are **9b** (PDB ID 4cpq) and **10a** (PDB ID 4cps), both having intermediate distances to the Asp125 carboxylate group (2.9 and 3.1 Å, respectively, cf. Supporting Information). The adjustment of the macrocyclic scaffold in the P1–P3 region is also reflected in the rotation of the isopropyl group at the S2 pocket (Figure 4), which includes the amino acid residues Ala28, Asp30, and Val184. In the linear PIs, the isopropyl group has a clear (**9a**, PDB ID 4cp7) or possible (**9b**, PDB ID 4cpq and **9e**, PDB ID 4cpr) orientation where the two methyl groups are situated closer to the Ala28 side chain. For the P1–P3 macrocyclic PIs, the isopropyl group

appears to be forced to point away from the nitrogen (**10a**, PDB ID 4cps; **10d**, PDB 4cpu; and **10e**, PDB ID 4cpx), as the isopropyl group is now closer to the backbone of the protein (cf. Supporting Information).

The terminal allylic groups in P1 and P3 position of the linear PIs do not seem to interact closely with the protein (Figure 3). Instead, the P3-allyl group is directed away from the protein surface and is assumed to be flexible. The same is true for the allylic extension in *para* position on the phenyl alanine mimicking group at P1 site, which has little or no defined density for those atoms. As for previously examined groups in P1' position with this scaffold, the rather large thiophene side chain is directed toward the surface of the protein. In almost all complexes examined so far, the conserved aromatic structure of the P1' side chain has a well-defined density, whereas the *para* substituted (hetero)aromatic substituent was only partially defined.

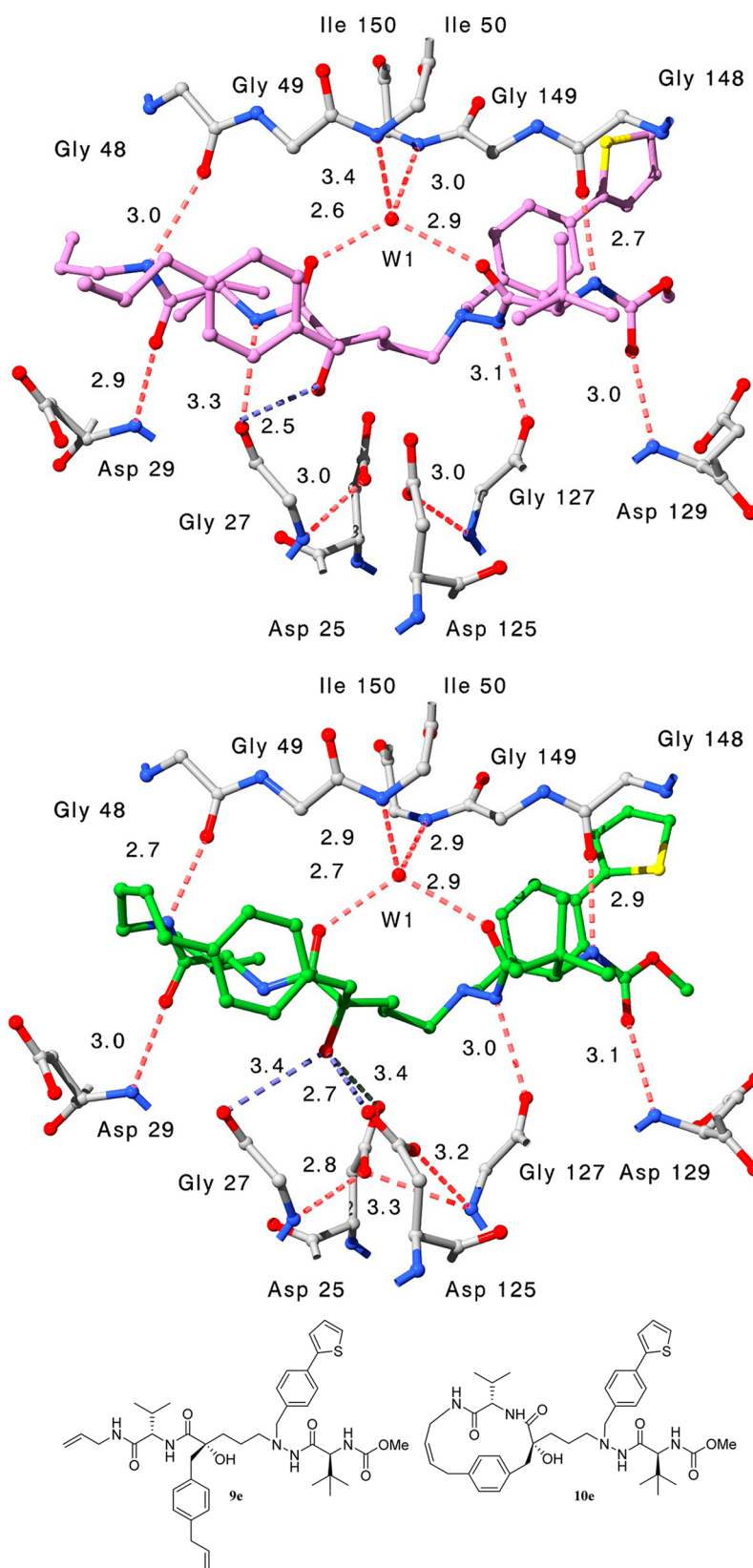


**Figure 4.** A close-up of the hydrogen bonding distances between the tertiary hydroxyl alcohol of the linear PI **9e** (top, pink, PDB ID 4cpr) and the macrocyclic PI **10e** (bottom, green, PDB ID 4cpx) and the catalytic residues Asp25/125, as well as the carbonyl oxygen of Gly27. The macrocyclic PI **10e** had hydrogen bond distances between the tertiary hydroxyl group and Asp125/25 of 2.7 and 3.4 Å, respectively. A contrasting scene is observed for the linear compounds **9e**, where the bonds to Asp125/25 are longer than 3.4 Å (not denoted in figure) and the bond to Gly27 is only 2.5 Å. The distance between the tertiary hydroxyl alcohol of the cyclic PI **10e** and the carbonyl oxygen of Gly27 is instead 3.4 Å.

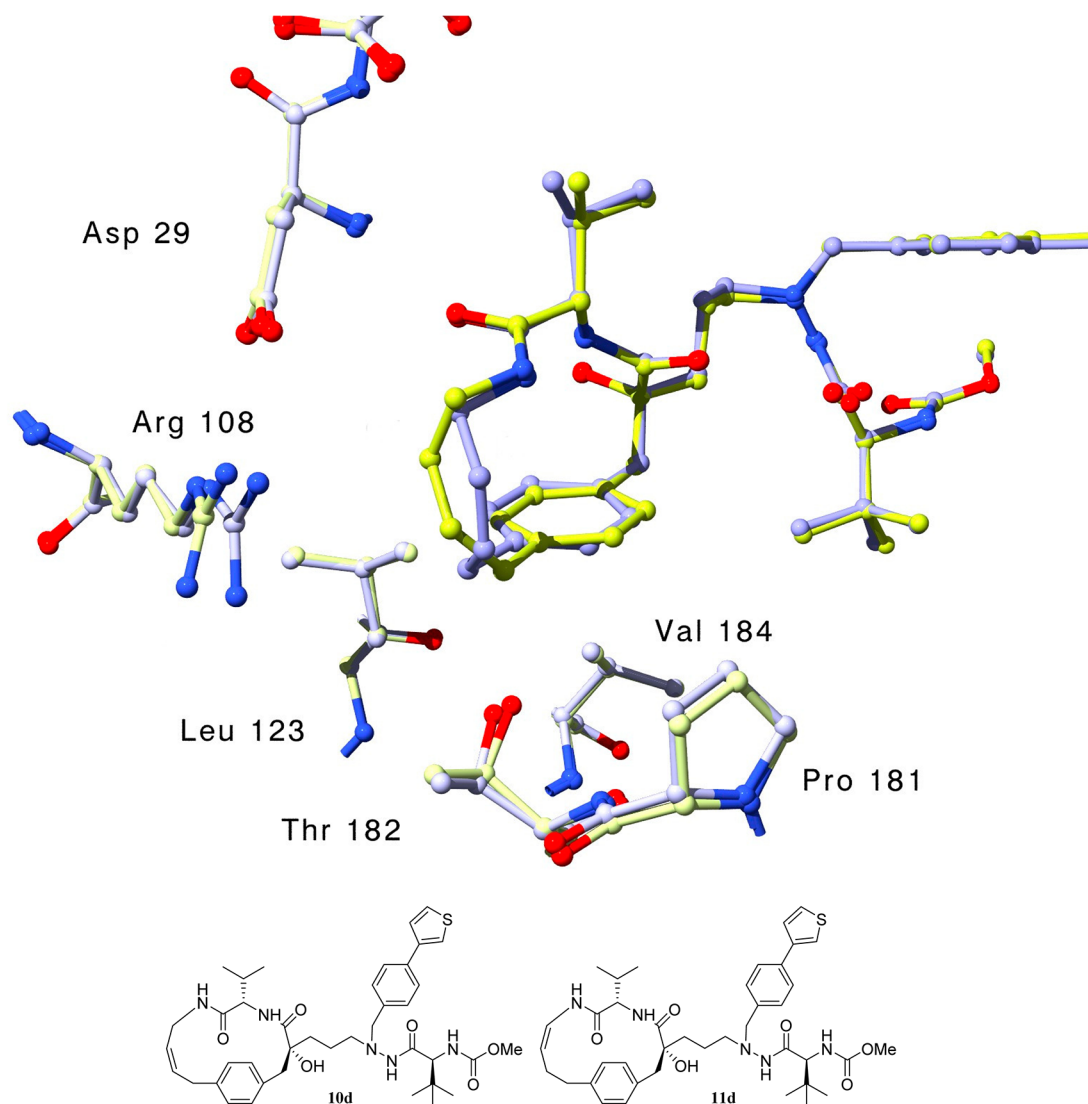


**Figure 5.** Structure of the complex protease enzyme/**10d** PI (blue, PDB ID 4cpu) is superimposed on the **11d** complex (yellow, PDB ID 4cpw).

Crystal structures of macrocycles having the same ring size (15 members) but with different double-bond position in the ring as a result of the double-bond migration during the RCM reaction, as mentioned in the Chemistry section, were also obtained. The restriction of the angles from the double bond causes this region to adapt different conformations. The electron density for PIs **10d** (PDB ID 4cpu) and **11d** (PDB ID 4cpw, Figure 5) could be confidently interpreted and shows that the region of the ring closure in PI **10d** is directed away from Arg108. In PI **11d**, on the other hand, it is pointing toward Arg108, causing the side chain to shift its position. For large size images and overview of all X-ray structures obtained, see Supporting Information.

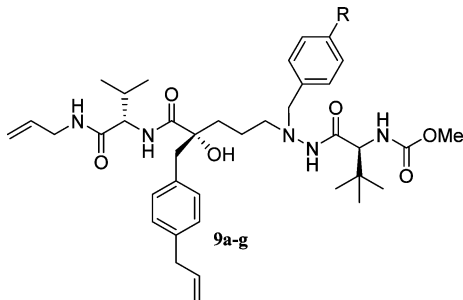
## CONCLUSION

In summary, 21 novel HIV-1 PIs have been synthesized. A set of seven linear new PIs encompassing a tertiary alcohol as part of the transition-state mimicking scaffold were obtained by decoration of the P1' site with (hetero)aromatic moieties. The P1' functionalization was in general beneficial as very good linear PIs were obtained. Almost all of them showed improved inhibition potency ( $K_i \leq 35$  nM) and better antiviral activity ( $EC_{50} \leq 3.7$   $\mu$ M) compared to the precursor phenyl bromide **A**

( $K_i$  30 nM and  $EC_{50}$  6.0  $\mu$ M), with **9a** ( $K_i$  7.8 nM,  $EC_{50}$  0.81  $\mu$ M) as the most potent linear PI. Fourteen macrocyclic PIs were obtained by a P1–P3 RCM reaction of the new linear HIV-1 PIs. Macrocyclic PIs exhibited  $EC_{50}$  values down to 0.13  $\mu$ M and  $K_i$  in the low nanomolar range ( $2.2$  nM  $\leq K_i \leq 120$  nM) combined with low cell toxicity and sufficient Caco-2 permeation. Overall, macrocyclization furnished a consistent improvement of antiretroviral activity, in many cases better than the precursor bromide **B**, with **10f** ( $K_i$  2.2 nM and  $EC_{50}$  0.2  $\mu$ M) as the most potent and promising macrocyclic PI of this new series.

## EXPERIMENTAL SECTION

**General Methods.**  $^1\text{H}$  and  $^{13}\text{C}$  NMR spectra were recorded on Varian Mercury Plus instruments:  $^1\text{H}$  at 399.9 MHz and  $^{13}\text{C}$  at 100.6 MHz at 25  $^\circ\text{C}$ . Analytical HPLC-MS was performed on a Gilson HPLC system with a Finnigan AQA quadrupole low-resolution mass spectrometer in positive or negative ESI mode using a Onyx Monolithic  $\text{C}_{18}$  4.6 mm  $\times$  50 mm 5  $\mu\text{m}$  (Phenomenex) or ACT C4 4.6 mm  $\times$  50 mm, 5  $\mu\text{m}$  column with MeCN in 0.05% aqueous HCOOH as mobile phase at a flow rate of 4 mL/min. Preparative HPLC-MS was performed on a Gilson HPLC equipped with a Zorbax SB-C8 (21.2 mm  $\times$  150 mm, Agilent Technologies) column or a 10  $\mu\text{m}$  Vydac C18 column (250 mm  $\times$  22 mm), in both cases with UV

**Table 1.** Enzyme Inhibition Data, Antiviral Activity, MT4 Cell Toxicity, Caco-2 Permeation, and Metabolic Stability of Linear PIs 9a–g


The chemical structure shows a linear peptidomimetic inhibitor with a central hydroxyl group, a piperazine ring, and various side chains including a piperidine ring, a benzyl group, and a carbamate group. The R group is defined in the table below.

Cmpd	R	$K_i$ (nM)	EC <sub>50</sub> ( $\mu$ M)	CC <sub>50</sub> ( $\mu$ M)	$P_{app}$ ( $\times 10^{-6}$ cm/s) <sup>c</sup>	$Cl_{int}$ ( $\mu$ g/min/mg) <sup>d</sup>
9a		7.8	0.81 3.5 <sup>e</sup> , > 50 <sup>f</sup>	> 50	22	73
9b		18	1.25	> 50	-	-
9c		65	3.7	> 50	-	-
9d		64	3.7	> 50	-	-
9e		35	2.4	> 50	-	-
9f		8	2.2 14.9 <sup>e</sup> , > 50 <sup>f</sup>	> 100	47	> 300
9g		12.5	1.1	35	27	-
A <sup>a</sup>	Br	30	6.0	24	16	-
atazanavir <sup>b</sup>		2.7	0.02 0.03 <sup>e</sup> , 0.04 <sup>f</sup>	24	5.3	90

<sup>a</sup>Bromide analogue of the linear PIs (PI 16a in an earlier paper).<sup>13</sup>

<sup>b</sup>Atazanavir was used as reference compound.<sup>37</sup> <sup>c</sup>Selected linear PIs were tested for Caco-2 cell permeation. <sup>d</sup>Selected linear PIs were tested for the metabolic stability. <sup>e</sup>Mutations in MT4/HIV-1 protease: A71V, I84V, L90M. <sup>f</sup>Mutations in MT4/HIV-1 protease: M46I, V82F, I84V.

detection at 220 nm, using MeCN in 0.05% aqueous HCOOH as mobile phase at a flow rate of 5 mL/min or MeCN in 0.1% aqueous TFA as mobile phase at a flow rate of 5 mL/min. Exact molecular masses were determined on Micromass Q-ToF2 mass spectrometer equipped with an electrospray ion source. Optical rotations were obtained on a PerkinElmer 241 polarimeter, specific rotations ( $[\alpha]_D$ )

are reported in deg/dm, and the concentration ( $c$ ) is given in g/100 mL in the specified solvent. The microwave reactions were performed in a Biotage Initiator producing controlled irradiation at 2450 MHz with a power of 0–300 W. Reaction temperatures were determined using the built-in online IR-sensor.

All PIs were >95% pure according to <sup>1</sup>H NMR, LC-UV (254 nm and 214 or 220 nm), and LC-MS (TIC).

**General Procedure of Ring Closing Metathesis for the Synthesis of Macrocylic PIs 10a–f, 11c–d, 11f–g, 12e, 13c, 13g, and 14f and Spectroscopic Data.** In a 2–5 mL process vial, to a solution of linear PI 9a–g (1.0 equiv) in anhydrous DCM (3 mL), second-generation Hoveyda–Grubbs catalyst (20 mmol %) was added under nitrogen flow. The vial was sealed then irradiated in the microwave reactor cavity at 130 °C for 1 h. After cooling to room temperature, the reaction mixture was filtered off through a plug of Celite, which was rinsed with ethyl acetate. The filtrate was evaporated under reduced pressure, giving the crude product, which was purified by preparative HPLC.

**Methyl ((S)-1-(2-(3-((3R,6S,Z)-3-Hydroxy-6-isopropyl-4,7-dioxo-5,8-diaza-1(1,4)-benzenacyclododecaphan-10-en-3-yl)-propyl)-2-(4-(pyridin-4-yl)benzyl)hydrazinyl)-3,3-dimethyl-1-oxobutan-2-yl)carbamate (10a).** PI 10a was prepared according to procedure E from 9a (14.5 mg, 0.0192 mmol) and second-generation Hoveyda–Grubbs catalyst (2.4 mg, 0.0038 mmol) in anhydrous DCM (3 mL). The crude product was purified by preparative HPLC, to give 8 mg of 10a as white solid, in 57% isolated yield. <sup>1</sup>H NMR (400 MHz, CD<sub>3</sub>OD):  $\delta$  8.59–8.57 (m, 2H), 7.71–7.67 (m, 4H), 7.56 (d,  $J$  = 8.3 Hz, 2H), 7.31 (dd,  $J$  = 7.9, 1.9 Hz, 1H), 7.11 (dd,  $J$  = 7.9, 1.9 Hz, 1H), 7.04 (dd,  $J$  = 7.9, 1.9 Hz, 1H), 6.88 (dd,  $J$  = 7.8, 1.9 Hz, 1H), 6.32 (dt,  $J$  = 10.3, 7.4 Hz, 1H) 5.69 (dt,  $J$  = 10.3, 7.2 Hz, 1H), 3.96 (s, 2H), 3.88–3.84 (m, 1H), 3.75–3.71 (m, 2H), 3.54 (s, 3H), 3.42 (t,  $J$  = 6.4 Hz, 1H), 2.87–2.82 (m, 4H), 2.10–1.98 (m, 2H), 1.95–1.83 (m, 3H), 1.80–1.68 (m, 2H), 0.80 (s, 9H), 0.78 (d,  $J$  = 6.7 Hz, 3H), 0.75 (d,  $J$  = 6.7 Hz, 3H). <sup>13</sup>C NMR (100 MHz, CD<sub>3</sub>OD):  $\delta$  176.03, 172.11, 171.89, 170.55, 150.56, 142.35, 137.85, 136.24, 135.34, 131.46, 131.41, 131.10, 129.33, 129.24, 128.15, 127.84, 123.06, 80.43, 62.43, 59.39, 58.76, 52.69, 38.12, 37.47, 34.94, 33.07, 32.83, 32.14, 30.77, 30.46, 26.91, 23.73, 19.89, 18.44. MS (ESI):  $m/z$  727 [M + H]<sup>+</sup> (100). HRMS  $m/z$  727.4186 [(M + H)<sup>+</sup> calcd for C<sub>41</sub>H<sub>55</sub>N<sub>5</sub>O<sub>6</sub><sup>+</sup> 727.4183].

**Methyl ((S)-1-(2-(3-((3R,6S,Z)-3-Hydroxy-6-isopropyl-4,7-dioxo-5,8-diaza-1(1,4)-benzenacyclododecaphan-10-en-3-yl)-propyl)-2-(4-(pyridin-3-yl)benzyl)hydrazinyl)-3,3-dimethyl-1-oxobutan-2-yl)carbamate (10b).** PI 10b was prepared according to procedure E from 9b (14 mg, 0.0185 mmol) and second-generation Hoveyda–Grubbs catalyst (2.3 mg, 0.0037 mmol) in anhydrous DCM (2 mL). The crude product was purified by preparative HPLC to give 7.3 mg of 10b as white solid in 54% isolated yield. <sup>1</sup>H NMR (400 MHz, CD<sub>3</sub>OD):  $\delta$  8.78–8.76 (m, 1H), 8.09–8.07 (m, 1H), 7.59–7.51 (m, 6H), 7.32 (dd,  $J$  = 7.9, 1.9 Hz, 1H), 7.12 (dd,  $J$  = 7.8, 1.9 Hz, 1H), 7.04 (dd,  $J$  = 7.9, 1.9 Hz, 1H), 6.88 (dd,  $J$  = 7.8, 1.9 Hz, 1H), 6.32 (dt,  $J$  = 10.4, 7.3 Hz, 1H) 5.74–5.67 (m, 1H), 3.96 (s, 2H), 3.87 (dd,  $J$  = 13.3, 9.6 Hz, 1H), 3.74–3.72 (m, 2H), 3.54 (s, 3H), 3.44–3.40 (m, 1H), 2.87–2.83 (m, 4H), 2.05–2.03 (m, 2H), 1.91–1.86 (m, 3H), 1.75–1.74 (m, 2H), 0.81 (s, 9H), 0.79 (d,  $J$  = 6.8 Hz, 3H), 0.75 (d,  $J$  = 6.7 Hz, 3H). <sup>13</sup>C NMR (100 MHz, CD<sub>3</sub>OD):  $\delta$  174.28, 171.80, 170.22, 169.98, 151.22, 140.72, 135.81, 134.62, 134.54, 133.54, 129.78, 129.60, 129.39, 127.64, 127.57, 126.38, 126.10, 105.55, 78.58, 57.90, 57.28, 56.67, 54.22, 36.28, 35.64, 33.23, 31.21, 29.74, 28.87, 28.61, 25.25, 21.90, 20.67, 18.19, 16.27. MS (ESI):  $m/z$  727 [M + H]<sup>+</sup> (100). HRMS  $m/z$  727.4175 [(M + H)<sup>+</sup> calcd for C<sub>41</sub>H<sub>55</sub>N<sub>6</sub>O<sub>6</sub><sup>+</sup> 727.4183].

**Methyl ((S)-1-(2-((1,1'-Biphenyl)-4-ylmethyl)-2-(3-((3R,6S,Z)-3-hydroxy-6-isopropyl-4,7-dioxo-5,8-diaza-1(1,4)-benzenacyclododecaphan-10-en-3-yl)propyl)hydrazinyl)-3,3-dimethyl-1-oxobutan-2-yl)carbamate (10c).** PI 10c was prepared according to procedure E from 9c (29 mg, 0.0385 mmol) and second-generation Hoveyda–Grubbs catalyst (4.8 mg, 0.0077 mmol) in anhydrous DCM (3.5 mL). The crude product was purified by preparative HPLC to give 3.6 mg (13%, isolated yield) of 10c as white solid, along with PIs 11c (10.0 mg, 36%, white solid) and 13c (2.9 mg, 10.5%, white solid), respectively.

Table 2. Enzyme Inhibition Data, Antiviral Activity, MT4 Cell Toxicity, Caco-2 Permeability, and Metabolic Stability of Macrocyclic PIs 10a–f, 11c–d, 11f–g, 12e, 13c, 13g, and 14f

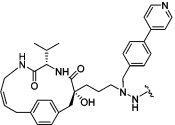
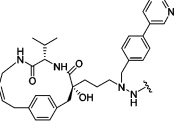
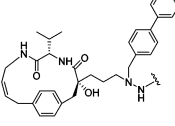
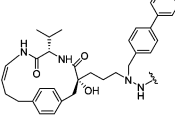
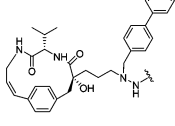
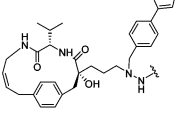
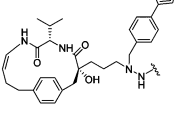
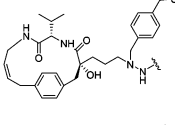
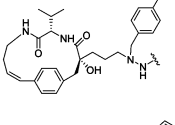
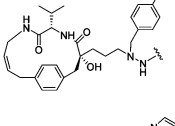
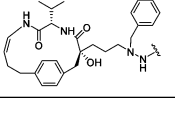
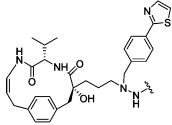
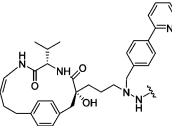
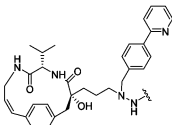
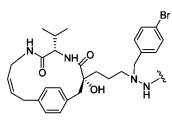
Cmpd	Structure	$K_i$ (nM)	$EC_{50}$ ( $\mu$ M)	$CC_{50}$ ( $\mu$ M)	$P_{app}$ ( $\times 10^{-6}$ cm/s) <sup>c</sup>	$Cl_{int}$ ( $\mu$ g/min/mg) <sup>d</sup>
10a		5.4	0.13 0.75 <sup>e</sup> , 3.0 <sup>f</sup>	> 50	< 1	> 300
10b		20	0.31 2.7 <sup>e</sup> , 9.4 <sup>f</sup>	> 50	-	-
10c		15	0.20 0.82 <sup>e</sup> , 2.85 <sup>f</sup>	41	-	-
11c		11	0.17	27	-	-
13c		22.5	1.15	64	-	-
10d		29.5	1.05	> 100	-	-
11d		31.5	1.08	> 100	-	-
10e		17	1	> 100	-	-
12e		120	7.35	> 100	-	-
10f		2.2	0.2 3.3 <sup>e</sup> , 13.5 <sup>f</sup>	> 100	2.2	> 300
11f		6.05	0.53	96	4.3	-

Table 2. continued

Cmpd	Structure	$K_i$ (nM)	$EC_{50}$ ( $\mu$ M)	$CC_{50}$ ( $\mu$ M)	$P_{app}$ ( $\times 10^{-6}$ cm/s) <sup>c</sup>	$Cl_{int}$ ( $\mu$ g/min/mg) <sup>d</sup>
14f		17	3.05	92	14	-
11g		3.6	0.19 1.25 <sup>e</sup> , 12.2 <sup>f</sup>	> 100	2	-
13g		9.1	0.77	96	7.8	-
B <sup>a</sup>		3.1	0.37	> 50	9	-
atazanavir <sup>b</sup>		2.7	0.02 0.032 <sup>e</sup> , 0.038 <sup>f</sup>	24	5.3	90

<sup>a</sup>Bromide analogue of the macrocyclic PIs (PI (R)-19a in an earlier paper).<sup>13</sup> <sup>b</sup>Atazanavir was used as reference compound.<sup>37</sup> <sup>c</sup>Selected macrocyclic PIs were tested for Caco-2 cell permeation. <sup>d</sup>Selected macrocyclic PIs were tested for the metabolic stability. <sup>e</sup>Mutations in MT4/HIV-1 protease: A71V, I84V, L90M. <sup>f</sup>Mutations in MT4/HIV-1 protease: M46I, V82F, I84V.

**10c:** <sup>1</sup>H NMR (400 MHz, CD<sub>3</sub>OD):  $\delta$  7.59–7.30 (m, 10H), 7.13–7.11 (m, 1H), 7.04–7.03 (m, 1H), 6.88 (dd,  $J = 7.8, 1.9$  Hz, 1H), 6.35–6.26 (m, 1H), 5.74–5.57 (m, 1H), 3.93 (s, 2H), 3.75–3.73 (m, 2H), 3.54 (s, 3H), 3.43–3.40 (m, 2H), 2.85–2.83 (m, 4H), 2.07–2.01 (m, 2H), 1.94–1.85 (m, 3H), 1.77–1.71 (m, 1H), 1.54–1.51 (m, 1H), 0.81 (s, 9H), 0.79 (d,  $J = 6.7$  Hz, 3H), 0.75 (d,  $J = 6.7$  Hz, 3H). <sup>13</sup>C NMR (100 MHz, CD<sub>3</sub>OD):  $\delta$  176.59, 172.24, 171.87, 166.38, 158.92, 142.37, 142.27, 141.66, 137.36, 136.26, 135.36, 131.42, 131.12, 129.81, 129.32, 129.25, 128.26, 127.90, 127.75, 87.11, 80.43, 63.07, 62.56, 58.61, 52.69, 38.13, 37.60, 34.96, 33.06, 32.83, 32.12, 30.74, 26.92, 23.72, 22.57, 19.89, 18.41. MS (ESI):  $m/z$  726 [M + H]<sup>+</sup> (100). HRMS  $m/z$  726.4238 [(M + H)<sup>+</sup> calcd for C<sub>42</sub>H<sub>56</sub>N<sub>5</sub>O<sub>6</sub><sup>+</sup> 726.4231].

**Methyl ((S)-1-(2-([1,1'-Biphenyl]-4-ylmethyl)-2-(3-((3R,6S,Z)-3-hydroxy-6-isopropyl-4,7-dioxo-5,8-diaza-1(1,4)-benzenacyclododecaphan-9-en-3-yl)propyl)hydrazinyl)-3,3-dimethyl-1-oxobutan-2-yl)carbamate (11c).** <sup>1</sup>H NMR (400 MHz, CD<sub>3</sub>OD):  $\delta$  7.59–7.40 (m, 9H), 7.34–7.30 (m, 2H), 7.27–7.19 (m, 1H), 6.95–6.90 (m, 1H), 6.45 (d,  $J = 9.2$  Hz, 1H), 4.96–4.93 (m, 1H), 3.95 (s, 2H), 3.73–3.70 (m, 1H), 3.54 (s, 3H), 3.49–3.45 (m, 1H), 2.88–2.79 (m, 4H), 2.48–2.40 (m, 1H), 2.19–2.16 (m, 1H), 2.09–1.84 (m, 5H), 1.60–1.52 (m, 2H), 0.84 (d,  $J = 6.8$  Hz, 3H), 0.81 (s, 9H), 0.79 (d,  $J = 6.6$  Hz, 3H). <sup>13</sup>C NMR (100 MHz, CD<sub>3</sub>OD):  $\delta$  176.26, 171.85, 171.24, 164.27, 158.92, 142.25, 141.73, 141.15, 135.78, 131.17, 129.81, 129.39, 129.29, 128.27, 127.91, 127.77, 123.17, 113.98, 110.53, 89.92, 80.87, 63.05, 62.64, 61.10, 58.68, 52.71, 47.22, 38.34, 35.98, 34.96, 30.74, 26.93, 22.53, 19.51, 19.44. MS (ESI):  $m/z$  726 [M + H]<sup>+</sup> (100). HRMS  $m/z$  726.4230 [(M + H)<sup>+</sup> calcd for C<sub>42</sub>H<sub>56</sub>N<sub>5</sub>O<sub>6</sub><sup>+</sup> 726.4231].

**Methyl ((S)-1-(2-([1,1'-Biphenyl]-4-ylmethyl)-2-(3-((3R,6S,Z)-3-hydroxy-6-isopropyl-4,7-dioxo-5,8-diaza-1(1,4)-benzenacyclododecaphan-9-en-3-yl)propyl)hydrazinyl)-3,3-dimethyl-1-oxobutan-2-yl)carbamate (13c).** <sup>1</sup>H NMR (400 MHz, CD<sub>3</sub>OD):  $\delta$  7.58–7.38 (m, 10H), 7.33–7.25 (m, 2H), 7.18 (dd,  $J = 7.8, 1.9$  Hz, 1H), 7.03–7.01 (m, 1H), 6.45 (d,  $J = 10.2$  Hz, 1H), 4.03 (d,  $J = 3.9$  Hz, 1H), 3.93 (s, 2H), 3.75–3.37 (m, 3H), 3.53 (s, 3H), 2.98 (d,  $J =$

13.1 Hz, 1H), 2.89–2.80 (m, 3H), 2.35–2.31 (m, 1H), 2.05–2.00 (m, 2H), 1.88–1.85 (m, 2H), 0.81 (s, 9H), 0.77 (d,  $J = 6.8$  Hz, 3H), 0.64 (d,  $J = 6.8$  Hz, 3H). <sup>13</sup>C NMR (100 MHz, CD<sub>3</sub>OD):  $\delta$  131.14, 129.81, 128.26, 127.89, 127.76, 121.70, 87.19, 80.98, 58.58, 52.68, 38.20, 36.12, 34.97, 30.45, 26.90, 20.10, 16.59. MS (ESI):  $m/z$  712 [M + H]<sup>+</sup> (100). HRMS  $m/z$  712.4072 [(M + H)<sup>+</sup> calcd for C<sub>41</sub>H<sub>54</sub>N<sub>5</sub>O<sub>6</sub><sup>+</sup> 712.4072].

**Methyl ((S)-1-(2-(3-((3R,6S,Z)-3-Hydroxy-6-isopropyl-4,7-dioxo-5,8-diaza-1(1,4)-benzenacyclododecaphan-10-en-3-yl)propyl)-2-(4-(thiophen-3-yl)benzyl)hydrazinyl)-3,3-dimethyl-1-oxobutan-2-yl)carbamate (10d).** PI 10d was prepared according to procedure E from 9d (11.3 mg, 0.0149 mmol) and second-generation Hoveyda–Grubbs catalyst (1.9 mg, 0.0030 mmol) in anhydrous DCM (2 mL). The crude product was purified by preparative HPLC to give 2.6 mg (24%) of 10d as white solid, along with the double-bond migration compound 11d, obtained as white solid in 4.4 mg, 40% isolated yield.

**10d:** <sup>1</sup>H NMR (400 MHz, CD<sub>3</sub>OD):  $\delta$  7.58–7.56 (m, 3H), 7.46–7.30 (m, 4H), 7.32 (dd,  $J = 7.9, 1.9$  Hz, 1H), 7.13–7.11 (m, 1H), 7.04 (dd,  $J = 7.8, 1.9$  Hz, 1H), 6.88 (dd,  $J = 7.8, 1.9$  Hz, 1H), 6.36–6.27 (m, 1H), 5.74–5.67 (m, 1H), 3.90 (s, 2H), 3.75–3.73 (m, 3H), 3.54 (s, 3H), 3.44–3.40 (m, 1H), 2.82 (m, 4H), 2.04–2.02 (m, 2H), 1.89–1.87 (m, 2H), 1.74–1.65 (m, 2H), 1.53–1.49 (m, 1H), 0.82 (s, 9H), 0.78 (d,  $J = 6.8$  Hz, 3H), 0.75 (d,  $J = 6.8$  Hz, 3H). <sup>13</sup>C NMR (100 MHz, CD<sub>3</sub>OD):  $\delta$  176.79, 174.38, 169.42, 164.55, 159.57, 157.14, 154.70, 139.96, 131.11, 127.10, 80.42, 68.80, 30.76, 26.93. MS (ESI):  $m/z$  732 [M + H]<sup>+</sup> (100). HRMS  $m/z$  732.3795 [(M + H)<sup>+</sup> calcd for C<sub>40</sub>H<sub>54</sub>N<sub>5</sub>O<sub>6</sub><sup>+</sup> 732.3795].

**Methyl ((S)-1-(2-(3-((3R,6S,Z)-3-Hydroxy-6-isopropyl-4,7-dioxo-5,8-diaza-1(1,4)-benzenacyclododecaphan-9-en-3-yl)propyl)-2-(4-(thiophen-3-yl)benzyl)hydrazinyl)-3,3-dimethyl-1-oxobutan-2-yl)carbamate (11d).** <sup>1</sup>H NMR (400 MHz, CD<sub>3</sub>OD):  $\delta$  7.58–7.56 (m, 3H), 7.46–7.24 (m, 4H), 7.25 (dd,  $J = 7.6, 1.8$  Hz, 1H), 7.08 (dd,  $J = 7.8, 1.6$  Hz, 1H), 6.95–6.90 (m, 2H), 6.45 (d,  $J =$

9.2 Hz, 1H), 4.96–4.94 (m, 1H), 3.90 (s, 2H), 3.72–3.70 (m, 1H), 3.55 (s, 3H), 3.47 (d,  $J = 10.1$  Hz, 1H), 2.81–2.79 (m, 4H), 2.48–2.30 (m, 3H), 2.19–2.18 (m, 1H), 1.92–1.88 (m, 3H), 1.87–1.58 (m, 2H), 0.85–0.82 (s, 12H), 0.78 (d,  $J = 6.7$  Hz, 3H).  $^{13}\text{C}$  NMR (100 MHz,  $\text{CD}_3\text{OD}$ ):  $\delta$  174.38, 171.88, 170.65, 164.58, 159.63, 157.11, 154.69, 152.24, 147.34, 143.37, 136.41, 131.12, 129.28, 127.22, 127.10, 127.06, 127.07, 110.58, 80.86, 63.06, 59.40, 58.59, 52.70, 38.38, 35.38, 34.97, 33.06, 30.74, 30.46, 26.93, 23.72, 19.50, 19.44. MS (ESI):  $m/z$  732  $[\text{M} + \text{H}]^+$  (100). HRMS  $m/z$  732.3791  $[(\text{M} + \text{H})^+]$  calcd for  $\text{C}_{40}\text{H}_{54}\text{N}_5\text{O}_6^+$  732.3795].

**Methyl ((S)-1-(2-(3-((3R,6S,Z)-3-Hydroxy-6-isopropyl-4,7-dioxo-5,8-diaza-1(1,4)-benzenacyclododecaphan-10-en-3-yl)-propyl)-2-(4-(thiophen-2-yl)benzyl)hydrazinyl)-3,3-dimethyl-1-oxobutan-2-yl)carbamate (10e).** PI 10e was prepared according to procedure E from 9e (20 mg, 0.0263 mmol) and second-generation Hoveyda–Grubbs catalyst (3.3 mg, 0.0053 mmol) in anhydrous DCM (3 mL). The crude product was purified by preparative HPLC to give 7.3 mg (34%) of 10e as white solid, along with the PI 12e, obtained as white solid in 2.5 mg, 13% isolated yield.

**10e:**  $^1\text{H}$  NMR (400 MHz,  $\text{CD}_3\text{OD}$ ):  $\delta$  7.55 (d,  $J = 8.2$  Hz, 2H), 7.42 (d,  $J = 8.2$  Hz, 2H), 7.43–7.35 (m, 3H), 7.14–7.07 (m, 3H), 6.89 (dd,  $J = 7.8, 1.9$  Hz, 1H), 6.33 (dt,  $J = 10.5, 7.3$  Hz, 1H), 5.75–5.68 (m, 1H), 3.91 (s, 2H), 3.76–3.73 (m, 2H), 3.57 (s, 3H), 3.44–3.41 (m, 2H), 2.85–2.82 (m, 4H), 2.06–2.02 (m, 1H), 1.95–1.85 (m, 2H), 1.77–1.72 (m, 1H), 1.62–1.48 (m, 3H), 0.83 (s, 9H), 0.80 (d,  $J = 6.8$  Hz, 3H), 0.76 (d,  $J = 6.8$  Hz, 3H).  $^{13}\text{C}$  NMR (100 MHz,  $\text{CD}_3\text{OD}$ ):  $\delta$  174.63, 170.71, 170.45, 162.84, 140.94, 134.84, 133.93, 133.55, 129.98, 129.79, 129.70, 127.90, 127.82, 127.65, 126.71, 125.07, 124.26, 122.66, 109.10, 88.50, 79.00, 61.64, 61.07, 57.96, 57.18, 51.30, 45.55, 36.71, 36.05, 33.53, 31.41, 30.68, 29.03, 25.51, 18.27, 16.98. MS (ESI):  $m/z$  732  $[\text{M} + \text{H}]^+$  (100). HRMS  $m/z$  732.3796  $[(\text{M} + \text{H})^+]$  calcd for  $\text{C}_{40}\text{H}_{54}\text{N}_5\text{O}_6\text{S}^+$  732.3795].

**Methyl ((S)-1-(2-(3-((3R,6S,Z)-3-Hydroxy-6-isopropyl-4,7-dioxo-5,8-diaza-1(1,4)-benzenacyclododecaphan-11-en-3-yl)-propyl)-2-(4-(thiophen-2-yl)benzyl)hydrazinyl)-3,3-dimethyl-1-oxobutan-2-yl)carbamate (12e).**  $^1\text{H}$  NMR (400 MHz,  $\text{CD}_3\text{OD}$ ):  $\delta$  7.55 (d,  $J = 7.9$  Hz, 2H), 7.42 (d,  $J = 7.9$  Hz, 2H), 7.36–7.26 (m, 3H), 7.10–7.07 (m, 3H), 6.94–6.91 (m, 1H), 6.46 (d,  $J = 9.1$  Hz, 1H), 5.36–5.34 (m, 1H), 3.68 (s, 5H), 3.58–3.48 (m, 4H), 2.38–2.30 (m, 2H), 2.25–2.20 (m, 2H), 2.07–2.03 (m, 2H), 1.65–1.59 (m, 5H), 0.91–0.83 (s, 15H).  $^{13}\text{C}$  NMR (100 MHz,  $\text{CD}_3\text{OD}$ ):  $\delta$  170.39, 164.26, 155.70, 149.16, 110.52, 89.91, 69.94, 64.36, 52.67, 34.94, 33.06, 30.75, 30.45, 30.45, 28.10, 26.93, 25.30, 23.72, 14.43. MS (ESI):  $m/z$  732  $[\text{M} + \text{H}]^+$  (100). HRMS  $m/z$  732.3790  $[(\text{M} + \text{H})^+]$  calcd for  $\text{C}_{40}\text{H}_{54}\text{N}_5\text{O}_6\text{S}^+$  732.3795].

**Methyl ((S)-1-(2-(3-((3R,6S,Z)-3-Hydroxy-6-isopropyl-4,7-dioxo-5,8-diaza-1(1,4)-benzenacyclododecaphan-10-en-3-yl)-propyl)-2-(4-(thiazol-2-yl)benzyl)hydrazinyl)-3,3-dimethyl-1-oxobutan-2-yl)carbamate (10f).** PI 10f was prepared according to procedure E from 9f (43 mg, 0.0565 mmol) and second-generation Hoveyda–Grubbs catalyst (7.0 mg, 0.0113 mmol) in anhydrous DCM (4 mL). The crude product was purified by preparative HPLC to give 7.7 mg (19% isolated yield) of 10f as white solid, along with two more PIs, 11f obtained as white solid in 2.0 mg (5% isolated yield) and PI 14f (2.6 mg, 6.5%, white solid), respectively.

**10f:**  $^1\text{H}$  NMR (400 MHz,  $\text{CD}_3\text{OD}$ ):  $\delta$  7.88–7.84 (m, 3H), 7.57 (d,  $J = 3.3$  Hz, 1H), 7.52 (d,  $J = 8.1$  Hz, 2H), 7.32 (dd,  $J = 8.0, 1.9$  Hz, 1H), 7.12 (dd,  $J = 7.9, 1.9$  Hz, 1H), 7.04 (dd,  $J = 7.9, 1.9$  Hz, 1H), 6.89 (dd,  $J = 8.0, 1.9$  Hz, 1H), 6.32 (dt,  $J = 10.6, 7.4$  Hz, 1H), 5.73–5.66 (m, 1H), 3.95 (s, 2H), 3.75–3.71 (m, 3H), 3.55 (s, 3H), 3.43–3.40 (m, 1H), 2.87–2.83 (m, 4H), 2.08–2.01 (m, 1H), 1.96–1.85 (m, 4H), 1.68–1.57 (m, 2H), 0.81–0.78 (m, 12H), 0.74 (d,  $J = 6.8$  Hz, 3H).  $^{13}\text{C}$  NMR (100 MHz,  $\text{CD}_3\text{OD}$ ):  $\delta$  176.07, 172.11, 171.89, 170.08, 158.88, 144.34, 142.36, 136.26, 135.34, 133.67, 131.41, 131.31, 131.11, 129.32, 129.24, 128.12, 127.35, 120.64, 80.43, 63.04, 62.38, 59.39, 58.80, 52.74, 46.97, 38.13, 37.48, 34.92, 33.06, 32.83, 32.11, 30.74, 26.91, 19.69, 18.41. MS (ESI):  $m/z$  733  $[\text{M} + \text{H}]^+$  (100). HRMS  $m/z$  733.3743  $[(\text{M} + \text{H})^+]$  calcd for  $\text{C}_{39}\text{H}_{53}\text{N}_5\text{O}_6\text{S}^+$  733.3747].

**Methyl ((S)-1-(2-(3-((3R,6S,Z)-3-Hydroxy-6-isopropyl-4,7-dioxo-5,8-diaza-1(1,4)-benzenacyclododecaphan-9-en-3-yl)-propyl)-2-(4-(thiazol-2-yl)benzyl)hydrazinyl)-3,3-dimethyl-1-**

**oxobutan-2-yl)carbamate (11f).**  $^1\text{H}$  NMR (400 MHz,  $\text{CD}_3\text{OD}$ ):  $\delta$  7.88–7.85 (m, 3H), 7.59–7.58 (m, 1H), 7.53 (d,  $J = 7.9$  Hz, 2H), 7.27–7.25 (m, 1H), 7.09–7.07 (m, 2H), 6.95–6.91 (m, 2H), 6.45 (d,  $J = 9.1$  Hz, 1H), 3.95 (s, 2H), 3.73–3.72 (m, 1H), 3.55 (s, 3H), 3.47 (d,  $J = 9.4$  Hz, 1H), 2.86–2.84 (m, 4H), 2.49–2.43 (m, 1H), 2.21–2.17 (m, 2H), 2.06–2.03 (m, 2H), 1.88–1.81 (m, 2H), 1.60–1.68 (m, 2H), 0.84 (d,  $J = 6.8$  Hz, 3H), 0.81–0.78 (m, 12H).  $^{13}\text{C}$  NMR (100 MHz,  $\text{CD}_3\text{OD}$ ):  $\delta$  176.23, 144.37, 131.34, 127.37, 120.64, 111.41, 80.88, 63.05, 52.74, 47.25, 38.36, 35.99, 34.93, 30.78, 26.91, 19. MS (ESI):  $m/z$  733  $[\text{M} + \text{H}]^+$  (100). HRMS  $m/z$  733.3742  $[(\text{M} + \text{H})^+]$  calcd for  $\text{C}_{39}\text{H}_{53}\text{N}_5\text{O}_6\text{S}^+$  733.3747].

**Methyl ((S)-1-(2-(3-((3R,6S,E)-3-Hydroxy-6-isopropyl-4,7-dioxo-5,8-diaza-1(1,4)-benzenacycloundecaphan-9-en-3-yl)-propyl)-2-(4-(thiazol-2-yl)benzyl)hydrazinyl)-3,3-dimethyl-1-oxobutan-2-yl)carbamate (14f).**  $^1\text{H}$  NMR (400 MHz,  $\text{CD}_3\text{OD}$ ):  $\delta$  7.88–7.85 (m, 4H), 7.59 (d,  $J = 3.3$  Hz, 1H), 7.55–7.53 (m, 3H), 7.27 (dd,  $J = 7.9, 1.9$  Hz, 1H), 7.19 (dd,  $J = 7.8, 2.0$  Hz, 1H), 7.03 (dd,  $J = 7.7, 1.9$  Hz, 1H), 6.45 (dt,  $J = 10.2, 2.4$  Hz, 1H), 4.03 (d,  $J = 3.9$  Hz, 1H), 3.96 (s, 2H), 3.55 (s, 3H), 3.49–3.47 (m, 1H), 3.00–2.91 (m, 2H), 2.88–2.82 (m, 4H), 2.36–2.31 (m, 2H), 2.05–2.00 (m, 3H), 0.81–0.77 (m, 12H), 0.65 (d,  $J = 6.9$  Hz, 3H).  $^{13}\text{C}$  NMR (100 MHz,  $\text{CD}_3\text{OD}$ ):  $\delta$  177.75, 144.36, 138.91, 137.16, 133.71, 132.27, 131.31, 130.47, 129.46, 127.37, 121.72, 120.65, 113.19, 112.66, 80.88, 66.99, 62.54, 61.05, 58.59, 52.71, 38.21, 36.14, 33.07, 31.07, 30.75, 26.91, 23.73, 22.67, 20.10, 16.59. MS (ESI):  $m/z$  719  $[\text{M} + \text{H}]^+$  (100). HRMS  $m/z$  719.3594  $[(\text{M} + \text{H})^+]$  calcd for  $\text{C}_{38}\text{H}_{51}\text{N}_6\text{O}_6\text{S}^+$  719.3591].

**Methyl ((S)-1-(2-(3-((3R,6S,Z)-3-Hydroxy-6-isopropyl-4,7-dioxo-5,8-diaza-1(1,4)-benzenacycloundecaphan-10-en-3-yl)-propyl)-2-(4-(pyridin-2-yl)benzyl)hydrazinyl)-3,3-dimethyl-1-oxobutan-2-yl)carbamate (11g).** PI 11g was obtained according to procedure E from 9g (38.5 mg, 0.0510 mmol) and second-generation Hoveyda–Grubbs catalyst (6.4 mg, 0.0100 mmol) in anhydrous DCM (3.5 mL). The crude product was purified by preparative HPLC to give 4.7 mg (13%) of 11g as white solid, along with PI 13g, obtained as white solid in 7.4 mg, 20% isolated yield.

**11g:**  $^1\text{H}$  NMR (400 MHz,  $\text{CD}_3\text{OD}$ ):  $\delta$  8.69–8.68 (m, 1H), 8.19–8.15 (m, 1H), 8.04–8.02 (m, 1H), 7.88 (d,  $J = 8.0$  Hz, 2H), 7.63–7.53 (m, 4H), 7.27 (dd,  $J = 7.8, 1.8$  Hz, 1H), 7.19 (dd,  $J = 7.8, 1.8$  Hz, 1H), 7.03 (dd,  $J = 7.7, 1.8$  Hz, 1H), 6.88 (d,  $J = 9.9$  Hz, 1H), 6.47–6.43 (m, 1H), 4.06–4.00 (m, 3H), 3.75–3.73 (m, 1H), 3.53 (s, 3H), 2.99 (d,  $J = 13.1$  Hz, 1H), 2.87–2.83 (m, 3H), 2.36–2.31 (m, 2H), 2.05–2.02 (m, 2H), 1.88–1.85 (m, 1H), 1.55–1.49 (m, 2H), 0.82 (s, 9H), 0.78 (d,  $J = 6.9$  Hz, 3H), 0.65 (d,  $J = 6.8$  Hz, 3H).  $^{13}\text{C}$  NMR (100 MHz,  $\text{CD}_3\text{OD}$ ):  $\delta$  178.86, 177.33, 171.89, 158.89, 157.20, 147.99, 138.88, 137.12, 132.24, 131.78, 131.29, 130.46, 129.44, 128.24, 124.61, 121.69, 112.84, 80.87, 68.85, 63.09, 62.53, 58.58, 52.67, 46.98, 38.20, 36.12, 34.95, 31.04, 30.72, 26.92, 23.71, 22.65, 20.10, 16.58. MS (ESI):  $m/z$  713  $[\text{M} + \text{H}]^+$  (100). HRMS  $m/z$  713.4033  $[(\text{M} + \text{H})^+]$  calcd for  $\text{C}_{40}\text{H}_{53}\text{N}_6\text{O}_6^+$  713.4027].

**Methyl ((S)-1-(2-(3-((3R,6S,Z)-3-Hydroxy-6-isopropyl-4,7-dioxo-5,8-diaza-1(1,4)-benzenacyclododecaphan-9-en-3-yl)-propyl)-2-(4-(pyridin-2-yl)benzyl)hydrazinyl)-3,3-dimethyl-1-oxobutan-2-yl)carbamate (13g).**  $^1\text{H}$  NMR (400 MHz,  $\text{CD}_3\text{OD}$ ):  $\delta$  8.79–8.77 (m, 1H), 8.50–8.46 (m, 1H), 8.25–8.24 (m, 1H), 7.90–7.85 (m, 3H), 7.71–7.66 (m, 2H), 7.23 (dd,  $J = 7.8, 1.8$  Hz, 1H), 7.13–7.04 (m, 2H), 6.95–6.91 (m, 1H), 6.45 (d,  $J = 9.3$  Hz, 1H), 4.97–4.95 (m, 1H), 4.08–4.01 (m, 2H), 3.75–3.73 (m, 2H), 3.53 (s, 3H), 2.89–2.79 (m, 4H), 2.49–2.40 (m, 1H), 2.04–2.02 (m, 2H), 1.89–1.75 (m, 3H), 1.60–1.58 (m, 3H), 0.85–0.83 (m, 12H), 0.79 (d,  $J = 6.8$  Hz, 3H).  $^{13}\text{C}$  NMR (100 MHz,  $\text{CD}_3\text{OD}$ ):  $\delta$  176.16, 171.90, 171.18, 158.88, 155.77, 145.72, 145.12, 141.16, 135.72, 135.18, 131.68, 131.63, 131.39, 129.38, 129.02, 128.67, 125.75, 123.14, 114.00, 80.87, 68.84, 63.09, 62.40, 58.80, 52.70, 47.22, 38.30, 35.96, 34.91, 33.12, 32.08, 30.72, 26.93, 22.59, 19.81, 19.42. MS (ESI):  $m/z$  727  $[\text{M} + \text{H}]^+$  (100). HRMS  $m/z$  727.4177  $[(\text{M} + \text{H})^+]$  calcd for  $\text{C}_{41}\text{H}_{55}\text{N}_6\text{O}_6^+$  727.4183].

## ■ ASSOCIATED CONTENT

### Supporting Information

Experimental details and spectroscopic data for all PIs, X-ray pictures, and structure determination details. This material is available free of charge via the Internet at <http://pubs.acs.org>.

## ■ AUTHOR INFORMATION

### Corresponding Author

\*Phone: +46 18 4714667. Fax: +46 18 4714474. E-mail: Mats.Larhed@orgfarm.uu.se.

### Notes

The authors declare no competing financial interest.

## ■ ACKNOWLEDGMENTS

MDR thanks Olaf van der Veen for his contribution to the synthetic work and Jean-Baptiste Véron for helpful discussions.

## ■ ABBREVIATIONS USED

AIDS, acquired immune deficiency syndrome; ART, antiretroviral therapy; HIV, human immunodeficiency virus; MIDA, N-methyliminodiacetic acid; PDB, Protein Data Bank; PI, protease inhibitor; MW, microwaves; RCM, ring-closing metathesis; SARs, structure–activity relationships

## ■ REFERENCES

- (1) Brun-Vezinet, F.; Charpentier, C. Update on the human immunodeficiency virus. *Med. Mal. Infect.* **2013**, *43* (5), 177–184.
- (2) Clavel, F.; Hance, A. J. HIV drug resistance. *N. Engl. J. Med.* **2004**, *350* (10), 1023–1035.
- (3) Sidibe, M. We need you beside us on the road to zero. *AIDS Care: Psychol. Socio-Med. Aspects AIDS/HIV* **2012**, *24* (8), 944.
- (4) Rusconi, S.; Scozzafava, A.; Mastrolorenzo, A.; Supuran, C. T. An update in the development of HIV entry inhibitors. *Curr. Top. Med. Chem.* **2007**, *7* (13), 1273–1289.
- (5) Hawkins, T. Understanding and managing the adverse effects of antiretroviral therapy. *Antiviral Res.* **2010**, *85* (1), 201–209.
- (6) Lin, J. H. Pharmacokinetics of biotech drugs: peptides, proteins and monoclonal antibodies. *Curr. Drug. Metab.* **2009**, *10* (7), 661–691.
- (7) Craik, D. J.; Fairlie, D. P.; Liras, S.; Price, D. The future of peptide-based drugs. *Chem. Biol. Drug. Des.* **2013**, *81* (1), 136–147.
- (8) Rezai, T.; Yu, B.; Millhauser, G. L.; Jacobson, M. P.; Lokey, R. S. Testing the conformational hypothesis of passive membrane permeability using synthetic cyclic peptide diastereomers. *J. Am. Chem. Soc.* **2006**, *128* (8), 2510–2511.
- (9) Meyer, F. M.; Collins, J. C.; Borin, B.; Bradow, J.; Liras, S.; Limberakis, C.; Mathiowetz, A. M.; Philippe, L.; Price, D.; Song, K.; James, K. Biaryl-bridged macrocyclic peptides: conformational constraint via carbogenic fusion of natural amino acid side chains. *J. Org. Chem.* **2012**, *77* (7), 3099–3114.
- (10) Pitsinos, E. N.; Vidali, V. P.; Couladouros, E. A. Diaryl ether formation in the synthesis of natural products. *Eur. J. Org. Chem.* **2011**, *2011* (7), 1207–1222.
- (11) Driggers, E. M.; Hale, S. P.; Lee, J.; Terrett, N. K. The exploration of macrocycles for drug discovery—an underexploited structural class. *Nature Rev. Drug Discovery* **2008**, *7* (7), 608–624.
- (12) Marsault, E.; Peterson, M. L. Macrocycles are great cycles: applications, opportunities, and challenges of synthetic macrocycles in drug discovery. *J. Med. Chem.* **2011**, *54* (7), 1961–2004.
- (13) Joshi, A.; Véron, J.-B.; Unge, J.; Rosenquist, Å.; Wallberg, H.; Samuelsson, B.; Hallberg, A.; Larhed, M. Design and synthesis of P1-P3 macrocyclic tertiary alcohol comprising HIV-1 protease inhibitors. *J. Med. Chem.* **2013**, *56* (22), 8999–9007.
- (14) Croom, K. F.; Dhillon, S.; Keam, S. J. Atazanavir: a review of its use in the management of HIV-1 infection. *Drugs* **2009**, *69* (8), 1107–1140.

(15) Wang, F.; Ross, J. Atazanavir: a novel azapeptide inhibitor of HIV-1 protease. *Formulary* **2003**, *38* (12), 691–702.

(16) (a) Ekegren, J. K.; Ginman, N.; Johansson, A.; Wallberg, H.; Larhed, M.; Samuelsson, B.; Unge, T.; Hallberg, A. Microwave-accelerated synthesis of P1'-extended HIV-1 protease inhibitors encompassing a tertiary alcohol in the transition-state mimicking scaffold. *J. Med. Chem.* **2006**, *49* (5), 1828–1832. (b) Ekegren, J. K.; Unge, T.; Safa, M. Z.; Wallberg, H.; Samuelsson, B.; Hallberg, A. A new class of HIV-1 protease inhibitors containing a tertiary alcohol in the transition-state mimicking scaffold. *J. Med. Chem.* **2005**, *48* (25), 8098–8102. (c) Wu, X.; Ohrgren, P.; Ekegren, J. K.; Unge, J.; Unge, T.; Wallberg, H.; Samuelsson, B.; Hallberg, A.; Larhed, M. Two-carbon-elongated HIV-1 protease inhibitors with a tertiary-alcohol-containing transition-state mimic. *J. Med. Chem.* **2008**, *51* (4), 1053–1057. (d) Mahalingam, A. K.; Axelsson, L.; Ekegren, J. K.; Wannberg, J.; Kihlstrom, J.; Unge, T.; Wallberg, H.; Samuelsson, B.; Larhed, M.; Hallberg, A. HIV-1 protease inhibitors with a transition-state mimic comprising a tertiary alcohol: improved antiviral activity in cells. *J. Med. Chem.* **2010**, *53* (2), 607–615. (e) Ohrgren, P.; Wu, X. Y.; Persson, M.; Ekegren, J. K.; Wallberg, H.; Vrang, L.; Rosenquist, A.; Samuelsson, B.; Unge, T.; Larhed, M. HIV-1 protease inhibitors with a tertiary alcohol containing transition-state mimic and various P2 and P1' substituents. *MedChemComm* **2011**, *2* (8), 701–709. (f) Wu, X. Y.; Ronn, R.; Gossas, T.; Larhed, M. Easy-to-execute carbonylations: microwave synthesis of acyl sulfonamides using Mo(CO)<sub>6</sub> as a solid carbon monoxide source. *J. Org. Chem.* **2005**, *70* (8), 3094–3098.

(17) Larhed, M.; Hoshino, M.; Hadida, S.; Curran, D. P.; Hallberg, A. Rapid fluorod Stille coupling reactions conducted under microwave irradiation. *J. Org. Chem.* **1997**, *62* (16), 5583–5587.

(18) Floistrup, E.; Goede, P.; Stromberg, R.; Malm, J. Synthesis of estradiol backbone mimics via the Stille reaction using copper(II) oxide as co-reagent. *Tetrahedron Lett.* **2011**, *52* (2), 209–211.

(19) Wu, X.; Ohrgren, P.; Joshi, A.; Trejos, A.; Persson, M.; Arvela, R. K.; Wallberg, H.; Vrang, L.; Rosenquist, A.; Samuelsson, B. B.; Unge, J.; Larhed, M. Synthesis, X-ray analysis, and biological evaluation of a new class of stereopure lactam-based HIV-1 protease inhibitors. *J. Med. Chem.* **2012**, *55* (6), 2724–2736.

(20) Nilsson, P.; Gold, H.; Larhed, M.; Hallberg, A. Microwave-assisted enantioselective Heck reactions: expediting high reaction speed and preparative convenience. *Synthesis* **2002**, *11*, 1611–1614.

(21) Larhed, M.; Hallberg, A. Microwave-promoted palladium-catalyzed coupling reactions. *J. Org. Chem.* **1996**, *61* (26), 9582–9584.

(22) Larhed, M.; Moberg, C.; Hallberg, A. Microwave-accelerated homogeneous catalysis in organic chemistry. *Acc. Chem. Res.* **2002**, *35* (9), 717–727.

(23) Kappe, C. O.; Dallinger, D. The impact of microwave synthesis on drug discovery. *Nature Rev. Drug Discovery* **2006**, *5* (1), 51–63.

(24) Callam, C. S.; Lowary, T. L. Suzuki cross-coupling reactions: synthesis of unsymmetrical biaryls in the organic laboratory. *J. Chem. Educ.* **2001**, *78* (7), 947–948.

(25) Miyaura, N.; Suzuki, A. Palladium-catalyzed cross-coupling reactions of organoboron compounds. *Chem. Rev.* **1995**, *95* (7), 2457–2483.

(26) Billingsley, K.; Buchwald, S. L. Highly efficient monophosphine-based catalyst for the palladium-catalyzed Suzuki–Miyaura reaction of heteroaryl halides and heteroaryl boronic acids and esters. *J. Am. Chem. Soc.* **2007**, *129* (11), 3358–3366.

(27) Tyrrell, E.; Brookes, P. The synthesis and applications of heterocyclic boronic acids. *Synthesis* **2003**, *4*, 469–483.

(28) Knapp, D. M.; Gillis, E. P.; Burke, M. D. A general solution for unstable boronic acids: slow-release cross-coupling from air-stable MIDA boronates. *J. Am. Chem. Soc.* **2009**, *131* (20), 6961–6963.

(29) Wu, X. Y.; Ekegren, J. K.; Larhed, M. Microwave-promoted aminocarbonylation of aryl iodides, aryl bromides, and aryl chlorides in water. *Organometallics* **2006**, *25* (6), 1434–1439.

(30) Bold, G.; Fassler, A.; Capraro, H. G.; Cozens, R.; Klimkait, T.; Lazdins, J.; Mestan, J.; Poncioni, B.; Rosel, J.; Stover, D.; Tinteln-Blomley, M.; Acemoglu, F.; Beck, W.; Boss, E.; Eschbach, M.; Hurlimann, T.; Masso, E.; Roussel, S.; Ucci-Stoll, K.; Wyss, D.; Lang,

R. New aza-dipeptide analogues as potent and orally absorbed HIV-1 protease inhibitors: candidates for clinical development. *J. Med. Chem.* **1998**, *41* (18), 3387–3401.

(31) Clavier, H.; Urbina-Blanco, C. A.; Nolan, S. P. Indenylidene ruthenium complex bearing a sterically demanding NHC ligand: an efficient catalyst for olefin metathesis at room temperature. *Organometallics* **2009**, *28* (9), 2848–2854.

(32) Rix, D.; Caijo, F.; Laurent, I.; Boeda, F.; Clavier, H.; Nolan, S. P.; Mauduit, M. Aminocarbonyl group containing Hoveyda–Grubbs-type complexes: synthesis and activity in olefin metathesis transformations. *J. Org. Chem.* **2008**, *73* (11), 4225–4228.

(33) Curchay, F. C.; Sworen, J. C.; Ghiviriga, I.; Abboud, K. A.; Wagener, K. B. Understanding structural isomerization during ruthenium-catalyzed olefin metathesis: a deuterium labeling study. *Organometallics* **2006**, *25* (26), 6074–6086.

(34) Schmidt, B. An olefin metathesis/double-bond isomerization sequence catalyzed by an in situ generated ruthenium hydride species. *Eur. J. Org. Chem.* **2003**, *5*, 816–819.

(35) Furstner, A.; Thiel, O. R.; Ackermann, L.; Schanz, H. J.; Nolan, S. P. Ruthenium carbene complexes with *N,N'*-bis(mesityl) imidazol-2-ylidene ligands: RCM catalysts of extended scope. *J. Org. Chem.* **2000**, *65* (7), 2204–2207.

(36) Lazorova, L.; Hubatsch, I.; Ekegren, J. K.; Gising, J.; Nakai, D.; Zaki, N. M.; Bergstrom, C. A. S.; Norinder, U.; Larhed, M.; Artursson, P. Structural features determining the intestinal epithelial permeability and efflux of novel HIV-1 protease inhibitors. *J. Pharm. Sci.* **2011**, *100* (9), 3763–3772.

(37) Robinson, B. S.; Riccardi, K. A.; Gong, Y. F.; Guo, Q.; Stock, D. A.; Blair, W. S.; Terry, B. J.; Deminie, C. A.; Djang, F.; Colonna, R. J.; Lin, P. F. BMS-232632, a highly potent human immunodeficiency virus protease inhibitor that can be used in combination with other available antiretroviral agents. *Antimicrob. Agents Chem.* **2000**, *44* (8), 2093–2099.